ELSEVIER

Journal of Nuclear Materials 241-243 (1997) 574-578

journal of nuclear materials

Study of carbon impurity generation by chemical sputtering in JT-60U

S. Higashijima *, H. Kubo, T. Sugie, K. Shimizu, N. Asakura, K. Itami, N. Hosogane, A. Sakasai, S. Konoshima, S. Sakurai, H. Takenaga

Japan Atomic Energy Research Institute, Naka-machi, Naka-gun, Ibaraki 311-01, Japan

Abstract

CD/CH-band intensities emitted from hydrocarbon molecules have been measured in the divertor region of JT-60U and the chemical sputtering yield of methane was estimated as a function of the surface temperature and the deuterium ion flux. The chemical sputtering yield increases with the surface temperature and decreases with increasing ion flux density in the L-mode plasmas. The B_4C converted CFC tiles are installed in JT-60U and it is found that the chemical sputtering of B_4C converted CFC tiles is suppressed in comparison to normal CFC tiles.

Keywords: JT-60U; Tokamak; Impurity source; Chemical erosion; Low Z wall material

1. Introduction

Reduction of carbon impurity generated by chemical sputtering processes is an important issue for the long operation scenario such as in ITER in order to reduce the erosion of the divertor tiles. Production of hydrocarbons is still important even if the electron temperature of the divertor plasma is so low that physical sputtering can be neglected. Chemical sputtering has been studied in many laboratories but has not been analyzed in the divertor machine except ASDEX UPGRADE [1].

In the previous experimental studies of impurity generation mechanism in JT-60U, it was concluded that carbon generation mechanism could be explained by deuterium, oxygen and carbon sputtering (physical sputtering) in high power ($\sim$ 22 MW) NB heating discharges and that the contribution of the chemical deuterium sputtering was small, but chemical oxygen sputtering was important [2,3]. But an analysis with a two-dimensional impurity code based on Monte Carlo techniques (IMPMC-code) showed that the profiles of C II intensity in the divertor region could not be explained without hydrocarbon molecule formation (e.g. methane CH_4 or CD_4) by chemical sputtering in high density discharges. This analysis also showed that methane generated at the private region due to chemical sputtering easily ionized near the X-point SOL region, which explains the remote radiative-cooling mechanism in the high density and MARFE operations [4]. In beam experiments it was reported that chemical sputtering strongly depended on the surface temperature of graphite materials [5]. Therefore a systematic study of the chemical sputtering dependence on the deuterium ion flux and the surface temperature has been performed in JT-60U.

2. Experiment

Hydrocarbons produced by chemical sputtering may include not only methane but also ethane, propane, etc., and ethylene which contains more than one carbon atom. So the lights emitted from hydrocarbon molecules were directly measured. Two typical C_2-band spectra of Swan system (transition: $A^3\Pi_g$–$X'^3\Pi_u$, vibrational state: (0, 0), wavelength: 516.5 nm and vibrational state: (1, 2), wavelength: 558.5 nm) [6,7] emitted from the C–C bond were not observed in divertor plasmas of JT-60U. Therefore it was summarized that the molecule formation with the C–C bond was small and can be neglected. In other words, CD/CH-band (transition: $A^2\Delta$–$X^2\Pi$, vibrational state: (0,

* Corresponding author.

PII S0022-3115(96)00567-3

0), wavelength: ~ 430.5 nm) spectrum emitted from the C–D or C–H bond of methane must be observed. Fig. 1 shows the spectrum of the CD/CH-band observed by the same spectrometer. In this experiment the concentration of oxygen impurity was below 0.5% of the electron density which was less than at the detection limit, indicating that the chemical sputtering by oxygen was negligible.

The spatial distribution of CD/CH-band intensity was measured with an absolutely calibrated multichannel filter spectrometer to estimate spatial profiles of methane flux generated from the divertor targets in JT-60U. This spectrometer divides the lights through a 38-channel optical fiber array into four parts (4 × 38 ch) and spatial profiles of four kinds of wavelength are analyzed along the same sight lines at the same time by interference filters. In this experiment CD/CH-band (wavelength: 430.5 nm), Bremsstrahlung (523.2 nm), C II (657.8 nm) and Dα/Hα (656.1 nm) intensities were measured. Since molecule spectrum width is wider than one of atom or ion, the component of Bremsstrahlung is especially considered to estimate the CD/CH-band intensity. For example, Bremsstrahlung intensity integrated from 429.5 nm to 431.0 nm in the CD/CH-band spectrum width became ~ 1/2 of measured CD/CH-band intensity in some discharges. Fig. 2 shows the diagnostics and plasma configuration in the divertor region in this experiment. On the divertor there are fifteen Langmuir probes and an IRTV camera measures the surface temperature of divertor tiles. Data in the region from the inner strike point to the outer strike point were measured in this plasma configuration. The chemical sputtering was analyzed at the positions of inboard two probes and outboard four probes (the closed circles in Fig. 2) with which the electron density, electron temperature, surface temperature and line intensities could be measured.

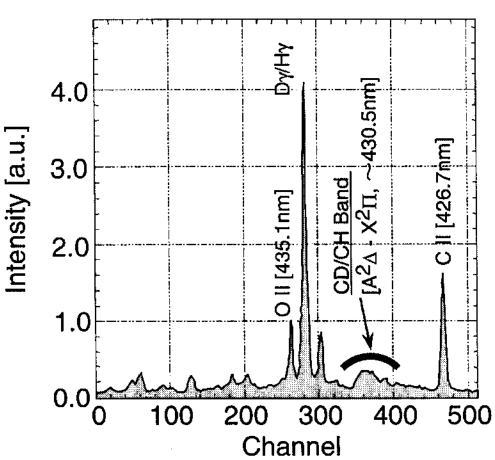

Fig. 1. The spectrum of the CD/CH-band observed by a spectrometer. O II, Dγ/Hγ and O II spectra were observed. In this series of experiment the level of oxygen impurity was below 0.5% of electron density, indicating that the chemical sputtering by oxygen could be neglected.

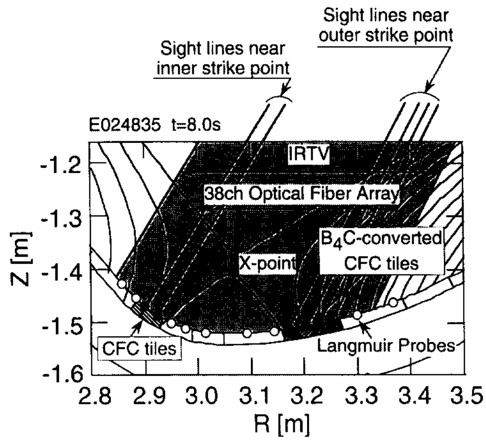

Fig. 2. Diagnostics and plasma configuration in the divertor region. Plasma parameters, line intensities, electron temperature, electron density and surface temperature, in the divertor region were measured with an absolutely calibrated 38-channel optical fiber array, fifteen Langmuir probes and an IRTV camera. In this experiment, the chemical sputtering flux was estimated at the location of inboard two probes and outboard four probes (closed circles).

The inner strike point was located on the carbon fiber composites (CFC) tiles and the outer strike point was located on the B_4C converted CFC tiles with the original thickness of B_4C layer of ~ 100 μm [8].

In this campaign high density L-mode plasmas with NB heating were analyzed. The discharge condition was as follows; $I_p = 1.2$ MA, $B_t = 3.5$ T, $q_{eff} \sim 7.0$, plasma vol-

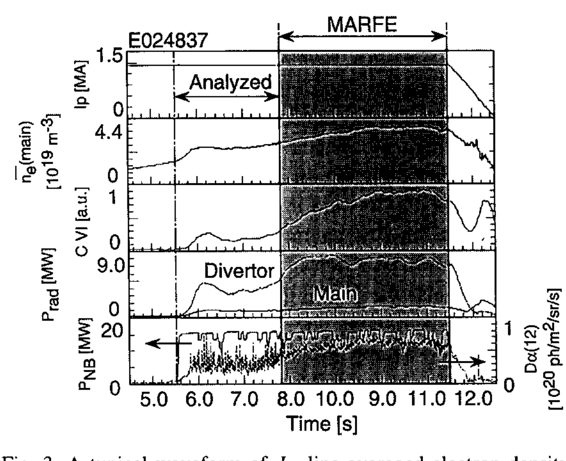

Fig. 3. A typical waveform of I_p, line averaged electron density, C VI intensity, radiation power in the main and divertor, NB injection power, Dα signal in the main plasma. I_p/B_t was 1.2 MA/3.5 T, $q_{eff} \sim 7.0$, the NB heating power was 4 MW ~ 22 MW, the averaged density was up to 4.5×10^{19} m^{-3} (~ MARFE) and the working gas was deuterium. In this discharge, NB heating was started at $t = 5.5$ s and a MARFE occurred at $t \sim 7.8$ s. When a MARFE started, C VI intensity in the main plasma and radiation in the divertor increased rapidly.

ume ~ 70 m^3, height of X-point ~ 0.14 m and the working gas was deuterium. To obtain chemical sputtering data in a wide range, it was attempted to reduce the vessel temperature from 300°C to 100°C that was the normal baking temperature of JT-60U. NB heating power was changed from 4 MW up to 22 MW and the line averaged density was increased up to 4.5×10^{19} m^{-3} ($\sim$ MARFE). A typical discharge is shown in Fig. 3. When a MARFE occurred, the C VI intensity in the main plasma increased and the radiation in the divertor increased. Since data of the Langmuir probes could not be measured when the densities were gradually increasing and plasma was detached, the data before the MARFE were analyzed.

3. Results

To estimate the chemical sputtering yield of methane from CD-band emission the following conditions were assumed.

(1) The S/XB values [9,10], representing the dissociation events or ionization events per photon, of C II, Dα and CD-band lines were used. But it is not clear whether these values can be applied to this experiment because these S/XB values were calculated under the low density limit and a more detailed estimation of atomic data may be necessary. In this experiment typically it is assumed that S/XB(C II) value is from ~ 1 ($T_e \sim 10$ eV) to ~ 54 ($T_e \sim 200$ eV), S/XB(Dα) is ~ 15 (10 eV $< T_e <$ 200 eV) and S/XB(CD-band) is from ~ 100 ($T_e \sim 10$ eV) to ~ 170 ($T_e \sim 100$ eV).

(2) As the concentration of oxygen impurity in the plasma was so small that the oxygen line signals of VUV spectrometer are noise levels, the carbon oxide sputtered chemically by oxygen was negligible.

(3) The signal of C_2-band light emitted from C–C bond was smaller than the detection limit of a spectrometer in this experiment, indicating that the hydrocarbon with more than two carbon atoms did not exit. The only hydrocarbon molecule generated by chemical sputtering was methane.

(4) Deuterium was rich in the plasma and hydrogen did not exist because the working gas had been only deuterium for the past six months and Hα was hidden by Dα and Hα intensity was not measured at all. The outflux to the divertor plates was only deuterium except carbon, a dominant impurity in JT-60U, and was calculated with Langmuir probe data. Because in this experiment the high density discharges up to the MARFE occurred densities were repeated and the deuterium recycling gradually increased shot by shot and deuterium ion outflux estimated from the Dα signals became considerably large, indicating that recycling rate is more than 1. Of course, the ion outfluxes calculated with the Langmuir probes were consistent with ones estimated from Dα signals in some early discharges.

(5) To calculate the ion outfluxes with the Langmuir probes, it was assumed that the sheath transmission factor was ~ 3 and the electron temperature was equal to the ion temperature. So the ion outflux is written as

$$\Gamma_{D^+} = n_e \sqrt{4T_e/m_i}\, \sin\theta,$$

m_i is deuterium ion mass and θ is the pitch angle of magnetic field line. To prevent from underestimating the Langmuir probe data, the only data before the MARFE were analyzed.

The surface temperature dependence of chemical sputtering yield analyzed at six Langmuir probe positions is shown in Figs. 4 and 5. Fig. 4(a) shows the data in the divertor density from 0.5×10^{19} m^{-3} to 1.0×10^{19} m^{-3} and Fig. 4(b) is from 1.0×10^{19} m^{-3} to 1.5×10^{19} m^{-3} near the inner strike point located on CFC tiles and in the electron temperature from 10 eV to 50 eV. Fig. 5(a) shows chemical sputtering yield near the outer strike point located on B_4C-converted CFC tiles in the same plasma parameters. The chemical sputtering yield of normal CFC tiles in Fig. 4 is monotonously increasing between 400 K and 600 K, but it is seemed that the yield of B_4C-converted CFC tiles is peaked at around 700 K. The change of surface temperature on divertor tiles near the inner strike

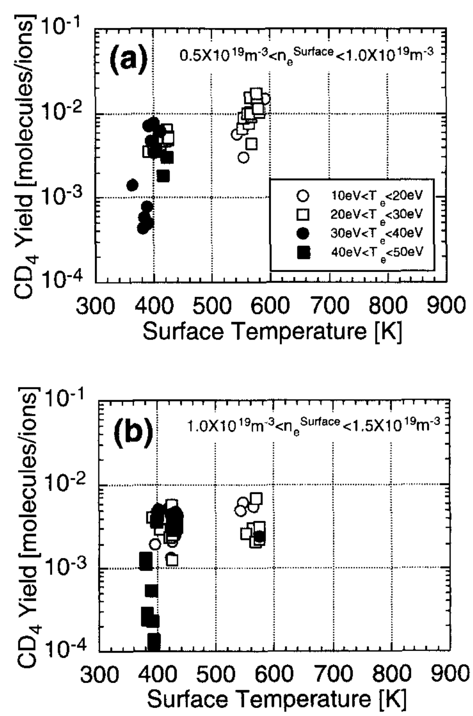

Fig. 4. Surface temperature dependence of chemical sputtering yield near the inner strike point located on CFC tiles (a) 0.5×10^{19} m^{-3} $< n_e^{surface} <$ 1.0×10^{19} m^{-3} and (b) 1.0×10^{19} m^{-3} $< n_e^{surface} <$ 1.5×10^{19} m^{-3}. The range of electron temperature in the divertor was from 10 eV to 50 eV and data are classified under 4 ranges of electron temperature up to 50 eV.

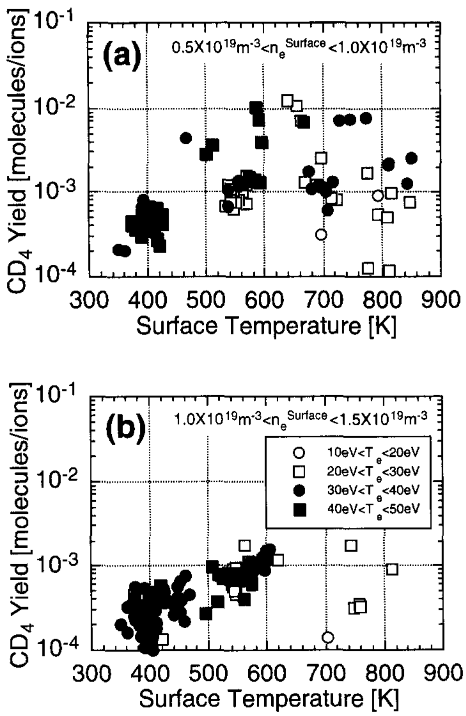

Fig. 5. Surface temperature dependence of chemical sputtering yield near the outer strike point located on B_4C converted CFC tiles (a) 0.5×10^{19} $m^{-3} < n_e^{surface} < 1.0\times10^{19}$ m^{-3} and (b) 1.0×10^{19} $m^{-3} < n_e^{surface} < 1.5\times10^{19}$ m^{-3}. The range of electron temperature in the divertor was from 10 eV to 50 eV.

point is small because particle flux usually goes to the inner strike point and in the contrary heat flux goes to the outer strike point in JT-60U. Though it is difficult to understand the dependence on electron density and electron temperature from these figures, chemical sputtering yield decreases with an increment of electron density and the dependence of electron temperature is not clear because chemical sputtering does not essentially depend on electron temperature in the range of the plasma parameters of JT-60U and because the errors of data are large. Chemical sputtering yield estimated with Dα intensity is almost the same maximum value but it has a tendency that data points largely scatter in the low yield region. It is because wall condition becomes worse and particle recycling is large. It is found that the chemical sputtering yield is larger near the inner strike point than one near the outer strike point. Especially it is prominent in the higher electron density case (1.0×10^{19}–1.5×10^{19} m^{-3}). It is due to different materials used for the divertor tiles. Eroded significantly through four years of operation, B_4C layer might be still effective in suppression of chemical sputtering. It was already reported that boron could suppress the chemical sputtering in a laboratory [11].

Fig. 6 indicates the deuterium ion flux dependence of chemical sputtering of normal CFC tiles. Fig. 6(a) shows

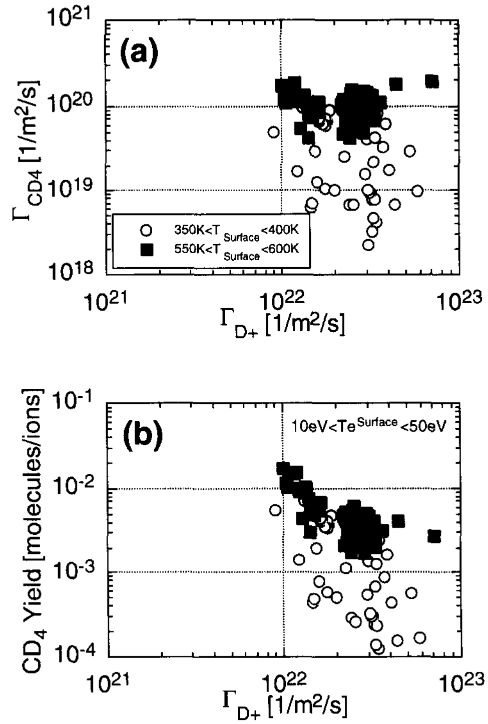

Fig. 6. The deuterium ion flux dependence of (a) methane flux and (b) chemical sputtering yield of methane at the location of CFC tiles near the inner strike point. The open circles represent data with the surface temperature of the divertor tiles from 350 K to 400 K and the open squares represent data with 550 K $< T_{surface}$ $<$ 600 K. Only data with 10 eV $< T_e <$ 50 eV are plotted to avoid the effect of physical sputtering.

the relation between sputtered methane flux and deuterium ion flux and Fig. 6(b) shows deuterium ion flux dependence of chemical sputtering yield. In these figures the

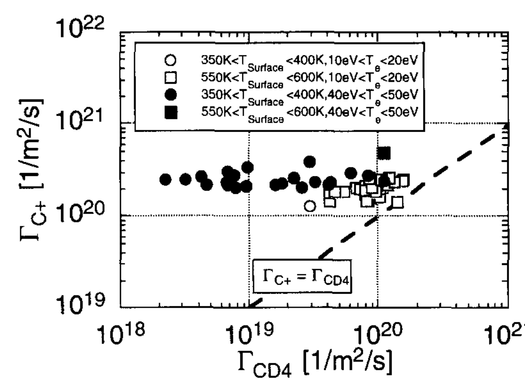

Fig. 7. C^+ flux versus CD_4. The open circles represent the data with 350 K $< T_{surface} <$ 400 K and the open squares indicate the data with 550 K $< T_{surface} <$ 600 K and in both cases only those data with 10 eV $< T_e <$ 20 eV are plotted. The closed circles represent the data with 350 K $< T_{surface} <$ 400 K and the closed squares indicate the data with 550 K $< T_{surface} <$ 600 K and T_e is from 40 eV to 50 eV.

data are plotted for two temperature ranges of the divertor tiles (350 K < $T_{surface}$ < 400 K, 550 K < $T_{surface}$ < 600 K). Only data were plotted with which the divertor electron temperature was between 10 eV and 50 eV to avoid the large effect of physical sputtering. In this experiment parameter region methane flux did not change with deuterium ion flux and with surface temperature of the CFC tiles. Even if deuterium ion flux increased by one order of magnitude, methane flux did not change and deuterium ion flux dependence of methane generation was small. As a result, chemical sputtering yield of methane decreased as deuterium ion flux increased as shown in Fig. 6(b). According to these results, in order to suppress chemical sputtering, the surface temperature of the tiles should be lowered, albeit associated with a larger ion flux.

In this experiment the profiles of C II intensity were also measured at the same time. The relation of C^+ flux and CD_4 flux at the inner strike point is shown in Fig. 7. This figure is plotted for four cases which is 350 K < $T_{surface}$ < 400 K or 550 K < $T_{surface}$ < 600 K and 10 eV < $T_e^{surface}$ < 20 eV or 40 eV < $T_e^{surface}$ < 50 eV. In this figure a dashed line shows C^+ flux is equal to CD_4 flux. C^+ flux does not change but CD_4 flux increased by two orders of magnitude. It found that the carbon generation process by chemical sputtering is especially dominant in the case of 350 K < $T_{surface}$ < 400 K and 10 eV < $T_e^{surface}$ < 20 eV.

4. Discussion

To estimate ion outflux, Langmuir probe data were used because L-mode high density discharges were repeated and wall condition became worse and worse. Under this situation particle recycling was larger and ion flux estimated with Dα signals might be an overestimation. In fact, data estimated from Dα signals have a tendency to scatter largely in the low yield region. In higher density the plasma is detached and MARFE occurs, the ion fluxes onto the divertor become smaller and data cannot be acquired by Langmuir probes. On the other hand, chemical sputtering could not be neglected by neutral particles, for example deuterium atoms, and a method to measure neutral particle flux in the divertor region is necessary for estimating chemical sputtering by neutral particles.

5. Conclusions

In the divertor region of JT-60U, CD-band intensity emitted from methane has been measured in L-mode high density plasma, and the chemical sputtering yield of methane was estimated as a function of surface temperature and deuterium ion flux. At the same time Bremsstrahlung, C II and Dα intensities were measured and the relations between the chemical sputtering and them were investigated. The conclusions are summarized as follows:

(1) The chemical sputtering yield of CFC tiles near the inner strike point is typically from 10^{-3} to 10^{-2} for 350 K < $T^{surface}$ < 600 K and 10 eV < $T_e^{surface}$ < 50 eV.

(2) The chemical sputtering of B_4C converted CFC tiles near the outer strike point is suppressed in comparison to normal CFC tiles. Especially the yield is $\sim 10^{-3}$ in the range of 350 K < $T^{surface}$ < 850 K and 10 eV < $T_e^{surface}$ < 50 eV and 1.0×10^{19} m^{-3} < $n_e^{surface}$ < 1.5×10^{19} m^{-3}.

(3) The chemical sputtering yield of methane generated from CFC tiles is decreased with an increment of deuterium ion flux and it changes from $\sim 10^{-2}$ to $\sim 10^{-3}$ when the deuterium ion flux changes from 1×10^{22} m^{-2} s^{-1} to 1×10^{23} m^{-2} s^{-1} between 10 eV < $T_e^{surface}$ < 50 eV.

Acknowledgements

The authors are grateful to JT-60U team for excellent cooperation. The authors would like to thank Dr. R. Yoshino, Dr. M. Azumi and Dr. H. Kishimoto for the continuous support. The authors would like to thank Dr. V. Phillips and Dr. A. Pospieszczyk for the useful discussions and advice.

References

[1] W. Poschenrieder et al., J. Nucl. Mater. 220–222 (1995) 36.
[2] H. Kubo et al., J. Nucl. Mater. 196–198 (1992) 71.
[3] A. Sakasai et al., IAEA Würzburg (1992) IAEA-CN-56/A-7-12.
[4] K. Shimizu et al., IAEA Seville (1994) IAEA-CN-60/D-P-I-2.
[5] J. Roth et al., Suppl. Nucl. Fusion 1 (1991) 64.
[6] A. Pospieszczyk et al., UCLA-PPG-1251 (1989).
[7] R.W.B. Pearse et al., The Identification of Molecular Spectra, 4th Ed. (Chapman and Hall Ltd., London, 1976).
[8] T. Ando et al., J. Nucl. Mater. 220–222 (1995) 375.
[9] K. Behringer, J. Nucl. Mater. 145–147 (1987) 145.
[10] K. Behringer, J. Nucl. Mater. 176–177 (1990) 606.
[11] C. García-Rosales et al., J. Nucl. Mater. 196–198 (1992) 573.